International Journal of Modern Physics B
Vol. 35, No. 27 (2021) 2150273 (14 pages)
© World Scientific Publishing Company
DOI: 10.1142/S0217979221502738

World Scientific
www.worldscientific.com

The visibility and stability of GaSe nanoflakes of about 50 layers on SiO_2/Si wafers

Ruslan A. Redkin[*,¶], Daniil A. Kobtsev[*,‖], Irina I. Kolesnikova[†,**], Svetlana Bereznaya[‡,††], Yury Sarkisov[§,‡‡], Vladimir Voevodin[‡,§§], Vadim Novikov[‡,¶¶], Timofei Mihaylov[†,‖‖] and Sergey Yu. Sarkisov[‡,***]

[*] *Laboratory of Optical Structures and Applied Photonics, R&D Center, Advanced Technologies in Microelectronics, Tomsk State University, 36 Lenin Avenue, Tomsk 634050, Russia*

[†] *Laboratory of Ionizing Radiation Detectors, R&D Center, Advanced Technologies in Microelectronics, Tomsk State University, 36 Lenin Avenue, Tomsk 634050, Russia*

[‡] *Laboratory for Terahertz Research, Tomsk State University, 36 Lenin Avenue, Tomsk 634050, Russia*

[§] *Department of Physics, Chemistry and Theoretical Mechanics, Tomsk State University of Architecture and Building, 2 Solyanaya Sq., Tomsk 634003, Russia*

[¶] *ruseg89@mail.ru*
[‖] *danbers27@gmail.com*
[**] *varsharova@mail.ru*
[††] *nlo.atom@mail.ru*
[‡‡] *sarkisov@tsuab.ru*
[§§] *voevodinvova2013@yandex.ru*
[¶¶] *novikovvadim@mail.ru*
[‖‖] *timofeu@mail2000.ru*
[***] *sarkisov@mail.tsu.ru*

Received 10 July 2021
Accepted 11 August 2021
Published 10 September 2021

GaSe nanoflakes on silicon substrates covered by SiO_2 films are prepared by mechanical exfoliation from the bulk Bridgman-grown GaSe crystals using a scotch tape. The thickness of SiO_2 films on Si substrates providing the highest optical contrast for observation of GaSe flakes is estimated by taking into account the spectral sensitivity of a commercial CMOS camera and broadband visible light illumination. According to our estimations, the optimal SiO_2 thickness is ∼126 nm for the visualization of GaSe flakes of 1–3 layers and ∼100 nm for the flakes of 40–70 layers. The obtained nanoflakes are investigated by optical and atomic force microscopy and Raman spectroscopy. The observed

[***]Corresponding author.

spectral positions of the Raman peaks are in agreement with the positions of the peaks known for bulk and nanolayered GaSe samples. It is found that the 50 nm thick flakes are stable but are covered by oxide structures with lateral size about 100 nm and height ∼5 nm after ∼9 months exposure to ambient atmosphere.

Keywords: Gallium selenide; nanoflakes; quasi-two-dimensional semiconductor; layered crystal; surface morphology; oxidation.

PACS numbers: 78.20.Ci, 81.65.Mq, 68.65.−k

1. Introduction

Currently, there has been a rapid increase in the number of works aimed at studying quasi-two-dimensional (2D) materials with new properties. A common feature of most 2D systems considered in the literature is the layered nature of the corresponding three-dimensional (3D) crystals.[1] For instance, among such 3D layered crystals are the well-known 2D transition metal dichalcogenides consisting of layers, each of which represents a set of three atomic planes in the sequence X–M–X (M = Mo, W; X = S, Se). Layers of the M_2X_3 type compounds (M = Bi, Sb; X = Se, Te) have a thickness of about 1 nm and include five atomic planes, in which atoms of groups V and VI sequentially alternate. The compounds of group III metal chalcogenides A^3B^6 (GaS, GaSe, InSe) are intermediate regarding the complexity of the layer arrangement compared to the two classes of materials mentioned above. Each layer of GaS, GaSe and InSe crystals is formed by four hexagonal atomic planes X–M–M–X (M = Ga, In; X = S, Se), i.e., two internal planes of metal atoms are sandwiched between the planes of S or Se atoms.[1,2]

Bulk GaS, GaSe, InSe and GaTe crystals are of practical interest in photovoltaics, nonlinear optics and modern electronics. Of these, GaSe crystals have largest applications. They were used in a number of works to generate monochromatic and broadband IR and terahertz radiation and to create IR sources for near-field IR nanoscopy systems, photo- and ionizing radiation detectors.[3–10]

Currently, nanolayered A^3B^6 structures have attracted the interest of researchers. Sufficiently large in their lateral dimensions, GaSe and GaS nanoflakes were first prepared by mechanical exfoliation and characterized using atomic force microscopy and Raman spectroscopy in Refs. 11 and 12. More recent experimental studies showed that GaSe nanolayers can be synthesized by the PVD method.[13,14] It was found that the photoconductivity and nonlinear optical susceptibilities of the second- and third-order of ultrathin GaSe layers increase per unit of thickness.[13–15] The possibility of patterned growth on substrates with pre-etched regions was shown, and samples deposited on transparent and flexible substrates were demonstrated.[12,16] A promising two-stage method for the fabrication of GaSe nanolayers was proposed, allowing synthesis of the nanolayers with lateral sizes up to 100 μm along with the possibility of controlling their thickness.[17,18] Measurements of photosensitivity already in the first studies clearly showed superiority in this parameter of GaSe layers (30 mA W^{-1} for the layers deposited on mica and 2.8 A W^{-1}

for samples produced by micromechanical cleavage) compared to pure graphene (1–6 mA W^{-1}) and monolayer MoS_2 (7.5 mA W^{-1}).[12,16] Another interesting feature of gallium chalcogenides, promising for spin devices, is the memory for polarization of the exciting radiation at photoluminescence that is associated with the presence of nondegenerate bands among the conduction and valence bands, separated from other states. The relaxation time of the spin polarization in GaSe is more than 500 ps and is achieved in the structures containing more than 100 layers.[19] Recently, the possibility of enhancing and controlling the polarized photoluminescence response from hybrid structures formed by GaSe nanoflakes on Si/SiO_2 substrates with an Ag nanoprism pattern on the top was reported.[20]

The nanolayered A^3B^6 structures have also been studied by computational quantum mechanics methods. The literature describes in detail problems with numerical modeling of the structural and electronic properties of layered and molecular crystals, in which the van der Waals forces play an important role.[21] The standard local density approximation and generalized gradient approximation within the framework of the density functional theory are not able to take into account dispersion interactions, which leads to significant errors in quantum chemical calculations. Application of recently developed van der Waals density functionals allows us to reduce the deviation of the theoretical values of layer thickness and interlayer distances in GaSe structure from the experimental data by an order of magnitude and brings this difference to an acceptable value of 0.2–1.9%.[22] Also, the binding energy in GaSe layers was estimated to be in the range of 14.2–16.2 meV $Å^{-2}$, which is slightly lower than the values for many layered metal chalcogenides estimated before.[22] The van der Waals functionals allow us to more accurately estimate the structural parameters of other III–VI structures as well.[23]

It is known that bulk GaSe crystals oxidize at humid atmosphere. The formation of oxide can be stimulated by illumination and usually initiates at selenium vacancies and dislocation edges.[24] In the case of nanolayered GaSe, the similar oxidation mechanisms take place.[25,26] From the first-principles calculations, it was revealed that perfect nanolayers are less prone to oxidation, while the nanolayers with chalcogen vacancies are much easier to oxidize.[25,26] It was reported that ultrathin few-layer flakes of GaSe can be completely decomposed in the atmosphere in a relatively short time.[27] Thus, for some applications, relatively thick nanoflakes of GaSe can be advantageous for practical use. Both photoresponse and nonlinear conversion efficiency increase per unit thickness. Therefore, it seems to be interesting to study preparation methods and stability of GaSe nanoflakes of several tens of layers.

The aim of the present study was to investigate the properties of 40–60 nm-thick GaSe nanoflakes, which correspond to ∼50–80 layers of GaSe. One of the addressed issues was the estimation of the thickness of SiO_2 films on Si substrates providing the highest optical contrast for observation of GaSe flakes by taking into account the spectral sensitivity of a commercial CMOS camera and broadband visible light illumination. Next, the stability of the nanoflakes in ambient atmosphere was investigated.

2. Experimental and Calculation Methods

The GaSe nanoflakes were prepared on the silicon substrates with (111) orientation. A silicon wafer was cut into 1×1 cm^2 substrates, which were degreased in toluene before deposition of the nanoflakes.

The SiO_2 films were deposited onto the Si substrates by magnetron sputtering using Si target and argon and oxygen gas flow in the chamber. The time of sputtering to produce the 100 nm-thick film was $t = 60$ s at the discharge voltage $U = 655$ V. During the optimization of the sputtering parameters, the thickness of the films was measured by AFM and an optical profilometer.

The structure of layers of GaSe and their stacking in bulk crystals are shown in Fig. 1. The sequence of atomic planes is Se–Ga–Ga–Se. Each metal atom in such a layer has tetrahedral surrounding of three Se atoms and one atom of Ga, while each Se atom is bonded to three Ga atoms. Strong covalent bonds within the layers and weak van der Waals interlayer binding with a small ion-covalent contribution led to strong anisotropy of the properties of A^3B^6 compounds. The thickness of the GaSe monolayer is $\sim$0.5 nm, while the interlayer distance is about 0.25 nm. The GaSe ingot 25 mm in diameter and 200 mm long was grown by the Bridgman method after synthesis in a two-zone horizontal furnace.[28] The slabs of the bulk material with a thickness of 300–600 μm were prepared by cleaving along the (0001) plane. The GaSe nanoflakes were deposited on SiO_2/Si substrates by mechanical exfoliation. The slab of the bulk material was peeled off by gluing an adhesive tape to its surface and then tearing it off. Then, by repeated gluing the tape to both sides of the sample and tearing to the sides, the sample was thinned to submicron sizes. After that, an adhesive tape with a thin layer of material was glued to the surface of the silicon substrate and then removed.

It is known that the interference between the rays reflected from the substrate and nanolayers can be used for better visualization of the latter.[29,30] We performed calculation of the dependence of the optical contrast produced by GaSe nanoflakes of thicknesses 0.5 nm (1 layer), 2 nm (3 layers), 7.25 nm (10 layers), 29.75 nm (40 layers) and 52.25 (70 layers) on the thickness of the SiO_2 films on Si substrates.

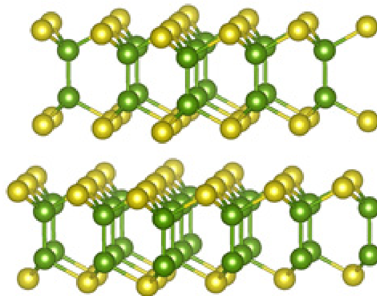

Fig. 1. (Color online) The structure of the layers of GaSe. The yellow spheres represent Se atoms, the green spheres represent Ga atoms.

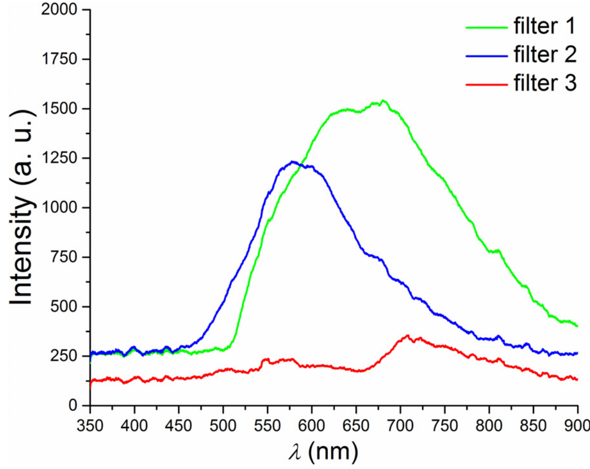

Fig. 2. (Color online) The measured intensity spectra of illumination by the light source of the microscope with filters 1–3.

The calculation was performed for observation under illumination by $\lambda = 555$ nm light (the wavelength of human eye maximum spectral sensitivity) and by a broadband visible light source with three different filters. The measured intensity spectra of illumination by the light source of the microscope with filters 1–3 are shown in Fig. 2. The calculation for the case of illumination by the light source of the microscope was performed by taking into account the spectral sensitivity of the camera.

The calculations of the optical contrast were performed in the following way. Due to the interference of the reflected rays (Fig. 3), the contrast $C(\lambda)$, obtained by observation with an optical microscope will be as follows:

$$C(\lambda) = \frac{\begin{array}{c}[(\mathrm{Re}(R_{\mathrm{nanolayer}}(\lambda)))^2 + (\mathrm{Im}(R_{\mathrm{nanolayer}}(\lambda)))^2] \\ -[(\mathrm{Re}(R_{\mathrm{SiO_2}}(\lambda)))^2 + (\mathrm{Im}(R_{\mathrm{SiO_2}}(\lambda)))^2]\end{array}}{[(\mathrm{Re}(R_{\mathrm{SiO_2}}(\lambda)))^2 + (\mathrm{Im}(R_{\mathrm{SiO_2}}(\lambda)))^2]}, \tag{1}$$

where the complex amplitude reflection coefficient from the SiO_2 layer is written as follows:

$$R_{SiO_2}(\lambda) = \frac{r_1 + r_2(\lambda)\exp(-2 \cdot i \cdot \varphi(\lambda))}{1 + r_1 r_2(\lambda)\exp(-2 \cdot i \cdot \varphi(\lambda))}, \tag{2}$$

where $\varphi(\lambda) = 2\pi \cdot n_{\mathrm{SiO_2}}(\lambda) d_{\mathrm{SiO_2}}/\lambda$, $r_1 = (1 - n_{\mathrm{SiO_2}}(\lambda))/(1 + n_{\mathrm{SiO_2}}(\lambda))$, $r_2(\lambda) = (n_{\mathrm{SiO_2}}(\lambda) - n_{\mathrm{Si}}(\lambda))/(n_{\mathrm{SiO_2}}(\lambda) + n_{\mathrm{Si}}(\lambda))$, $d_{\mathrm{SiO_2}}$ is a thickness of the SiO_2 layer, $n_{\mathrm{SiO_2}}(\lambda)$ is the wavelength dependence of the refractive index of SiO_2 and $n_{\mathrm{Si}}(\lambda)$ is the wavelength dependence of the refractive index of Si. The complex amplitude reflection coefficient of the nanolayer-SiO_2–Si structure is written as follows:

$$R_{\mathrm{nanolayer}}(\lambda) = \frac{r_1 \exp(i \cdot \varphi_1(\lambda)) + R'(\lambda)\exp(-i \cdot \varphi_1(\lambda))}{\exp(i \cdot \varphi_1(\lambda)) + r_1 R'(\lambda)\exp(-i \cdot \varphi_1(\lambda))}, \tag{3}$$

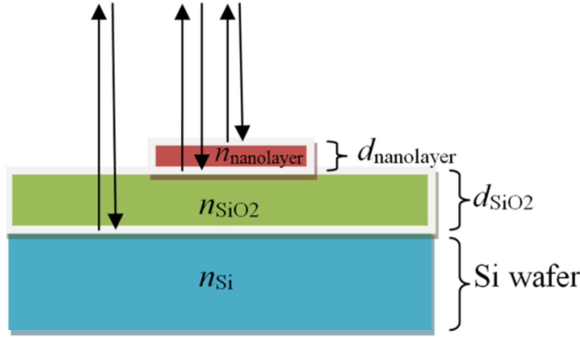

Fig. 3. (Color online) Visualization of nanolayers on the surface of a silicon substrate.

where

$$
\begin{aligned}
R'(\lambda) &= \frac{r_2 \exp(i \cdot \varphi_2(\lambda)) + r_3'(\lambda) \exp(-i \cdot \varphi_2(\lambda))}{\exp(i \cdot \varphi_2(\lambda)) + r_2'(\lambda) \cdot r_3'(\lambda) \exp(-i \cdot \varphi_2(\lambda))}, \qquad (4)\\
\varphi_1(\lambda) &= 2\pi \cdot n_{\text{nanolayer}}(\lambda) d_{\text{nanolayer}}/\lambda,\\
\varphi_2(\lambda) &= 2\pi(\lambda) = 2\pi \cdot n_{\text{SiO}_2}(\lambda) d_{\text{SiO}_2}/\lambda,\\
r_1' &= (1 - n_{\text{nanolayer}}(\lambda))/(1 + n_{\text{nanolayer}}(\lambda)),\\
r_2'(\lambda) &= (n_{\text{nanolayer}}(\lambda) - n_{\text{SiO}_2}(\lambda))/(n_{\text{nanolayer}}(\lambda) + n_{\text{SiO}_2}(\lambda)),\\
r_3'(\lambda) &= (n_{\text{SiO}_2}(\lambda) - n_{\text{Si}}(\lambda))/(n_{\text{SiO}_2}(\lambda) + n_{Si}(\lambda)),
\end{aligned}
$$

where $d_{\text{nanolayer}}$ is the thickness of the nanolayer and $n_{\text{nanolayer}}(\lambda)$ is the wavelength dependence of the refractive index of the nanolayer.

The optical contrast for the case of broadband visible light illumination and image registration by a camera with spectral sensitivity $S(\lambda)$ was calculated as follows:

$$
C'(\lambda) = \frac{\begin{array}{c}\int_{380\ \text{nm}}^{740\ \text{nm}} [(\text{Re}(R_{\text{nanolayer}}(\lambda)))^2 + (\text{Im}(R_{\text{nanolayer}}(\lambda)))^2 \\ -\, (\text{Re}(R_{\text{SiO}_2}(\lambda)))^2 + (\text{Im}(R_{\text{SiO}_2}(\lambda)))^2] \cdot S(\lambda) \cdot I(\lambda) d\lambda\end{array}}{\int_{380\ \text{nm}}^{740\ \text{nm}} [(\text{Re}(R_{\text{SiO}_2}(\lambda)))^2 + (\text{Im}(R_{\text{SiO}_2}(\lambda)))^2] \cdot S(\lambda) \cdot I(\lambda) d\lambda}, \qquad (5)
$$

where $I(\lambda)$ is the intensity spectrum of the illumination.

The refractive index values of GaSe nanoflakes were assumed to be as those for the bulk crystal. The spectral dependence of complex dielectric permittivity for an ordinary wave in bulk GaSe in the spectral region of 250–900 nm was taken from Ref. 31. It was used to calculate the refractive index spectral dependence. To get the analytical expression for $n_{\text{SiO}_2}(\lambda)$, the data from Ref. 32 in spectral region 200–1500 nm were approximated by formula (6):

$$
n(\lambda) = \left(1 + A\frac{\lambda^2}{\lambda^2 - B} + C\frac{\lambda^2}{\lambda^2 - D} + E\frac{\lambda^2}{\lambda^2 - F}\right)^{0.5}. \qquad (6)
$$

Analogously, the analytical expression for $n_{\text{Si}}(\lambda)$ was obtained by approximation by formula (6) of the data from Ref. 33 in the spectral region of 380–1450 nm.

The prepared nanoflakes were observed through optical microscope Altami MET 3, Altami, Russia, equipped with the digital color camera FL3-U3-32S2C-CS, Point Grey Research Inc., Canada.

The Raman spectra were measured by a Renishaw InVia Basis Raman spectrometer, Zeiss, Germany. The Raman spectra were excited at a wavelength of 532 nm.

The AFM images were measured by a Solver HV atomic force microscope, NT-MDT, Russia.

3. Results and Discussion

The thickness of SiO_2 films on Si substrates providing the highest optical contrast for observation of GaSe nanoflakes of different thickness was estimated for two different observation conditions. The calculated dependence of the optical contrast $C(\lambda)$ (formula (1)) produced by GaSe nanoflakes of 1, 3, 10, 40 and 70 layers on thicknesses of the SiO_2 films on Si substrates is shown in Fig. 4.

It can be seen (Fig. 4) that the highest positive contrast for thick flakes of 40–70 layers is achieved for the SiO_2 film thicknesses of 95, 284 and 473 nm. For the nanoflakes of 1–3 layers, thicker SiO_2 films are required (∼115, 305 and 493 nm).

Taking into account that in our experiments the observation was made by the Altami MET 3 optical microscope equipped with various color filters and a digital color CMOS camera, we also performed the calculations by assuming the actual illumination intensity spectra (Fig. 2) and spectral sensitivity of the camera. The resulting optical contrast $C'(\lambda)$ (formula (5)) for GaSe nanoflakes of 1, 3, 10, 40 and 70 layers on thicknesses of the SiO_2 films on Si substrates is shown in Fig. 5.

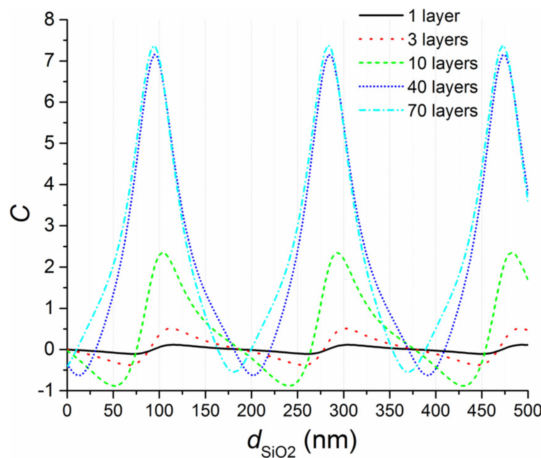

Fig. 4. (Color online) The optical contrast produced by GaSe nanoflakes of different thicknesses on Si/SiO_2 substrates under the illumination by $\lambda = 555$ nm light versus thickness of the SiO_2 film.

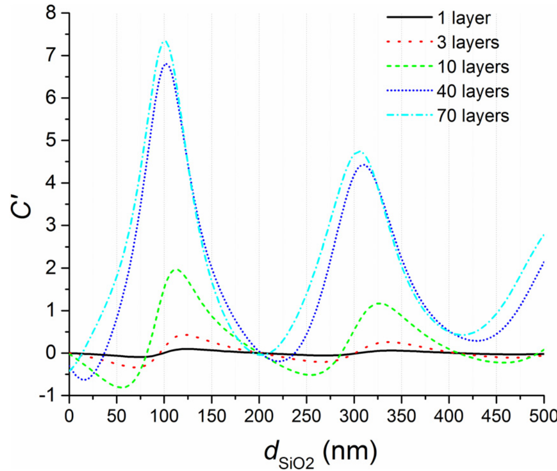

Fig. 5. (Color online) The optical contrast produced by GaSe nanoflakes of different thicknesses on Si/SiO_2 substrates under the illumination by the microscope light source with applied filter 1 (see spectrum in Fig. 2) and registration by the digital color camera.

In this case, the highest positive contrast for thick flakes of 40–70 layers is achieved for the SiO_2 film thicknesses of 100 and 473 nm (Fig. 5). For ultrathin flakes of 1–3 layers, the SiO_2 films of 126 and 340 nm thickness are required to provide the highest positive contrast. The calculated optical contrast $C'(\lambda)$ (formula (5)) for GaSe nanoflakes of 70 layers under illumination by the microscope light source with applied filters 1–3 and registration by the digital color camera is shown in Fig. 6. In this case, the highest positive contrast is achieved at $\sim$95 nm thick SiO_2 films (with applied filters 2 and 3), the local maxima at 290 and 493 nm being lower in C' values (Fig. 6). For the observation under illumination by the microscope light source with applied filter 1, thicker SiO_2 films of 100 and 306 nm are preferable.

Thus, the account for the actual experimental illumination spectrum (with maximum spectral intensity at 680 nm wavelength) and camera spectral sensitivity (with maximum spectral sensitivity at 535 nm wavelength) gives larger values of SiO_2 film thickness required for the highest optical contrast. Also, it gives decreased values of the contrast for the second and subsequent local maxima corresponding to thicker SiO_2 films, the contrast values at the first maximum (the thinnest possible SiO_2 film) being close to these at monochromatic light illumination and without taking into account the detector sensitivity spectrum.

According to our calculations, the best contrast produced by 40–60 nm thick GaSe nanoflakes on Si/SiO_2 substrates under the illumination by the microscope light source with applied filter 1 and registration by the digital color camera is provided in SiO_2 films with a thickness of 100 nm. The SiO_2 films of this thickness were deposited by magnetron sputtering. The optical images of GaSe nanoflakes deposited onto Si wafers with 100 nm thick SiO_2 films under the illumination by the microscope light source with applied filters 1–3 are shown in Fig. 7. The method of

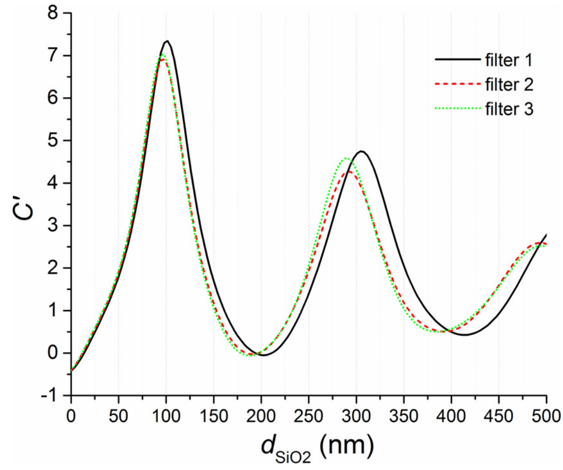

Fig. 6. (Color online) The optical contrast produced by GaSe nanoflakes of 70 layers on Si/SiO_2 substrates under the illumination by the microscope light source with applied filters 1, 2 and 3 (see spectra in Fig. 2) and registration by the digital color camera.

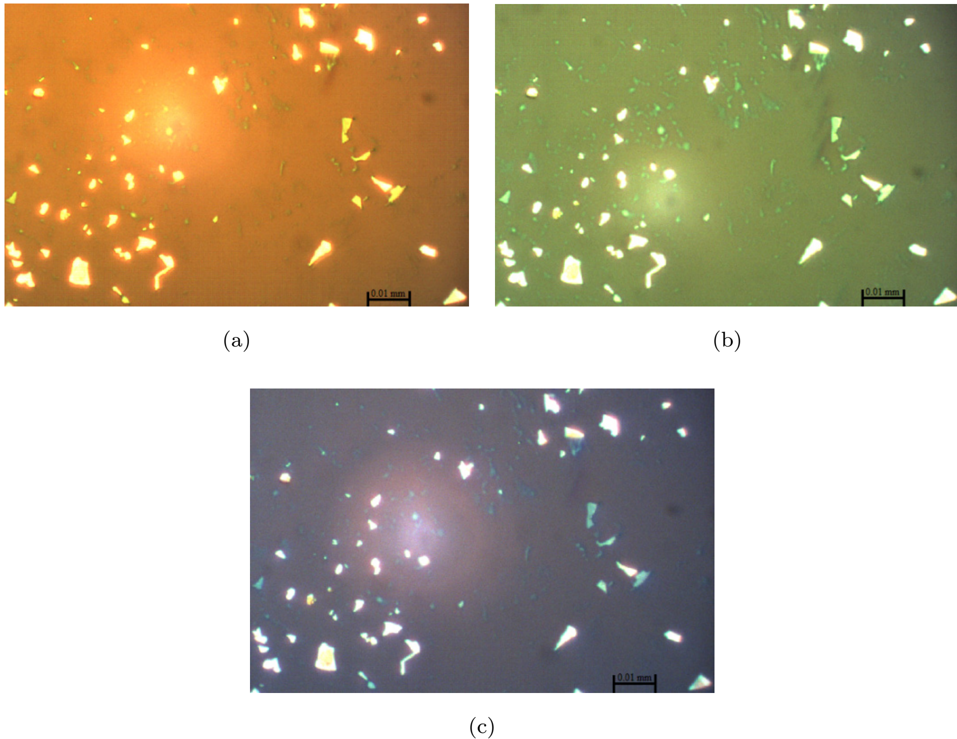

(a)

(b)

(c)

Fig. 7. (Color online) Optical microphotographs of Si wafer with deposited 100 nm-thick SiO_2 film and GaSe nanoflakes on the top under the illumination by the microscope light source with applied (a) filter 1, (b) filter 2 and (c) filter 3, registered by the digital camera.

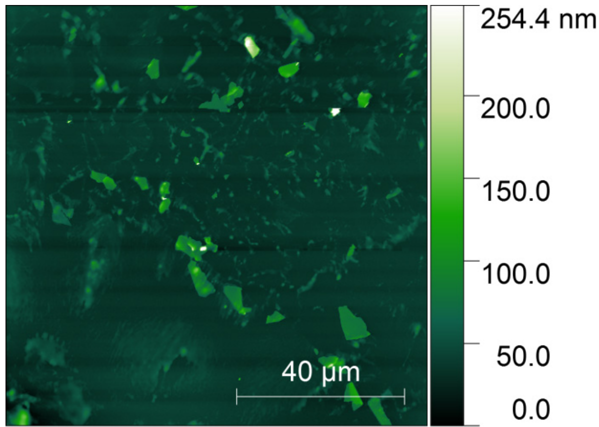

Fig. 8. (Color online) The AFM topology image for the as-prepared GaSe nanoflakes on a Si/SiO_2 substrate.

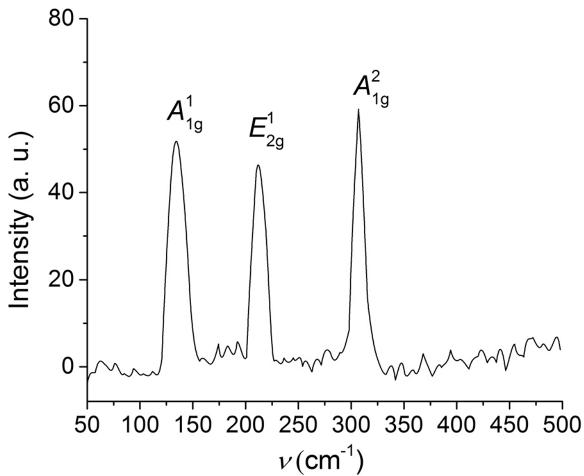

Fig. 9. Raman spectrum of a GaSe nanoflake of ∼70 layers.

mechanical exfoliation produces nanoflakes of various thicknesses. Nevertheless, the AFM investigation showed that the majority of the flakes had a thickness within 40–60 nm (Fig. 8). The nanoflakes of this thickness are seen with highest contrast on the images (Fig. 7). On each image (Fig. 8), nanoflakes with lower contrast are seen. The lateral sizes of the observed objects do not exceed 10 μm (Figs. 7 and 8).

The observed nanoscale objects belonging to the GaSe phase were confirmed by analyzing the Raman spectra (Fig. 9). It is well known that GaSe has D_{3h} symmetry and 12 vibrational modes, of which eight modes include vibrations in the plane of the layers (E' and E'') and four modes include vibrations perpendicular to the planes of the layers (A_1' and A_2''). The Raman-active vibrational modes are

sensitive to layer thickness (number of layers) and can be used to analyze it. The recorded Raman spectrum for a GaSe nanoflake of ~70 layers which shows three intense peaks at frequencies of 134 cm^{-1} (A^1_{1g}), 212 cm^{-1} (E^1_{2g}) and 307 cm^{-1} (A^2_{1g}) is shown in Fig. 9. The registered peak positions are in good agreement with the previously published data for bulk and nanolayered GaSe, according to which the indicated peaks lie at 132 cm^{-1} (A^1_{1g}), 211 cm^{-1} (E^1_{2g}) and 308 cm^{-1} (A^2_{1g}).[18] As is known from the previously published data, the peaks A^1_{1g} and E^1_{2g} for thinner GaSe nanolayers become less intense and almost disappear for the few-layer structures, while the A^2_{1g} peak remains the most intense and shifts to lower frequencies with decreasing layer thickness.[18,34] The analyzed nanoflake was rather thick, and the intensity of the peaks A^1_{1g} and E^1_{2g} is only slightly lower than the intensity of A^2_{1g} (Fig. 9).

In order to study the stability of the obtained nanoflakes, topology of their surfaces was studied by AFM just after preparation and after 9-month exposure to an ambient atmosphere. The AFM data for the as-prepared GaSe nanoflakes on

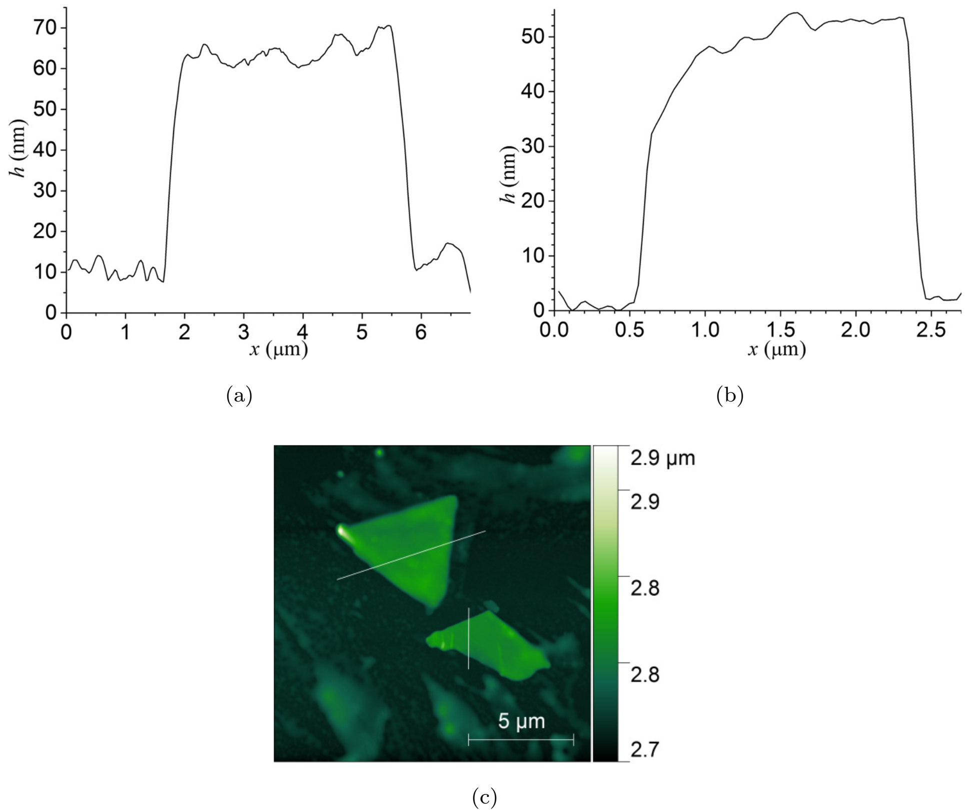

Fig. 10. (Color online) The AFM data for the as-prepared GaSe nanoflakes on Si/SiO_2 wafer: (a) and (b) - and height profiles along the white lines, shown on the surface morphology image in panel (c).

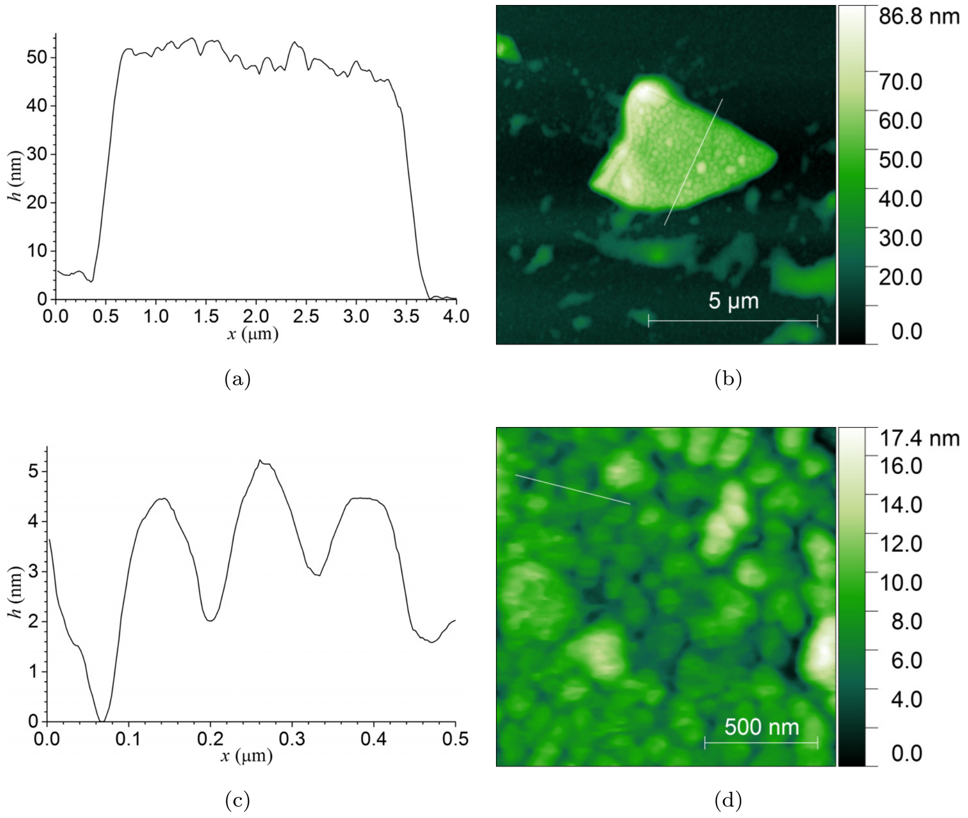

Fig. 11. (Color online) The AFM data for GaSe nanoflakes on Si/SiO_2 wafers after 9-month exposure to ambient atmosphere: (a), height profile along the white line, shown on the $10 \times 10\ \mu m^2$ surface morphology image in panel (b); (c) and height profile along the white line, shown on the $1,5 \times 1,5\ \mu m^2$ surface morphology image in panel (d).

Si/SiO_2 wafers are shown in Fig. 10. Two flakes are seen with lateral sizes of $\sim$5 μm and heights about 50–55 nm.

The AFM data for the GaSe nanoflakes on the same Si/SiO_2 wafer after 9-month exposure to the ambient atmosphere are shown in Fig. 11.

During the indicated time, the changes in shape and thickness of the nanoflakes on this substrate were not observed. Thus, the decomposition of the prepared GaSe nanoflakes of 40–70 layers in ambient atmosphere was not observed. On the other hand, comparing the surface morphology images presented in Figs. 10(c), 11(b) and 11(d), one can clearly see that new oxide structures are formed on the surface of the nanoflakes after 9-month exposure to ambient atmosphere. The nanoflakes are covered by oxide structures with lateral size of $\sim$100 nm and height of $\sim$5 nm after (Fig. 11). Nevertheless, these structures are not expected to influence the optical properties of the nanoflakes strongly on the contrary to the case of few-layer GaSe sheets. Taking into account higher general photosensitivity and nonlinear frequency

conversion efficiency of the thicker nanoslabs, this makes them advantageous for a number of practical optical devices compared to few-layer GaSe nanoflakes.

4. Conclusions

In conclusion, GaSe nanoflakes on silicon substrates covered by SiO_2 films were prepared by mechanical exfoliation from the bulk Bridgman-grown GaSe crystals using a scotch tape. The optical contrast produced by GaSe nanoflakes of 1, 3, 10, 40 and 70 layers depending on thickness of the SiO_2 films on Si substrates was calculated by taking into account the spectral sensitivity of a commercial CMOS camera and actual illumination spectrum. The higher visibility of the nanoflakes is strongly desirable, for example, at Raman or AFM measurements, as it makes the finding of the object to analyze easier. Also, optical methods of control are faster and simpler compared to more time-consuming, complicated and invasive AFM or TEM techniques. According to our estimations, the optimal SiO_2 thickness is $\sim$126 nm for the visualization of GaSe flakes of 1–3 layers and $\sim$100 nm for the flakes of 40–70 layers. The obtained nanoflakes were investigated by optical and atomic force microscopy and Raman spectroscopy. The observed spectral positions of the Raman peaks were in agreement with the positions of the peaks known for bulk and nanolayered GaSe samples. It was found that the 50 nm-thick flakes are stable but are covered by oxide structures with lateral size of $\sim$100 nm and height of $\sim$5 nm after 9-month exposure to ambient atmosphere. The decomposition of the prepared GaSe nanoflakes of 40–70 layers in ambient atmosphere was not observed. Taking into account the higher general photosensitivity and nonlinear frequency conversion efficiency, this makes such "thick" nanolayered structures advantageous for practical optical devices compared to few-layer GaSe nanoflakes.

Acknowledgments

This research was supported by the Ministry of Science and Higher Education of the Russian Federation, project No 0721-2020-0038.

References

1. F. Wang *et al.*, *Nanotechnol.* **26**, 292001 (2015).
2. A. Gouskov *et al.*, *Prog. Cryst. Growth Charact.* **5**, 323 (1982).
3. F. Keilmann and S. Amarie, *J. Infrared Millim. Terahertz Waves* **33**, 479 (2012).
4. R. Hegenbarth *et al.*, *Opt. Lett.* **37**, 3513 (2012).
5. W. Shi *et al.*, *Opt. Lett.* **27**, 1454 (2002).
6. F. Junginger *et al.*, *Opt. Lett.* **35**, 2645 (2010).
7. S. A. Bereznaya *et al.*, *J. Opt.* **19**, 115503 (2017).
8. R. A. Redkin *et al.*, *Mater. Res. Exp.* **6**, 126201 (2019).
9. R. Hegenbarth *et al.*, *J. Opt.* **16**, 094003 (2014).
10. Y. Toshinari *et al.*, *Jpn. J. Appl. Phys.* **32**, 1857 (1993).
11. D. J. Late *et al.*, *Adv. Funct. Mater.* **22**, 1894 (2012).
12. P.-A. Hu *et al.*, *ACS Nano* **6**, 5988 (2012).

13. S. Lei *et al.*, *Nano Lett.* **13**, 2777 (2013).
14. X. Zhou *et al.*, *J. Am. Chem. Soc.* **137**, 7994 (2015).
15. L. Karvonen *et al.*, *Sci. Rep.* **5**, 10334 (2015).
16. Y. Zhou *et al.*, *ACS Nano* **8**, 1485 (2014).
17. M. Mahjouri-Samani *et al.*, *ACS Nano* **8**, 11567 (2014).
18. M. Mahjouri-Samani *et al.*, *Adv. Funct. Mater.* **24**, 6365 (2014).
19. Y. Tang *et al.*, *Phys. Rev. B* **91**, 195429 (2015).
20. W. Wan *et al.*, *ACS Appl. Mater. Interfaces* **11**, 19631 (2019).
21. J. Klimeš and A. Michaelides, *J. Chem. Phys.* **137**, 120901 (2012).
22. S. Y. Sarkisov *et al.*, *J. Solid State Chem.* **232**, 67 (2015).
23. A. V. Kosobutsky and S. Yu. Sarkisov, *Phys. Sol. State* **60**, 1686 (2018).
24. S. A. Bereznaya *et al.*, *Infrared Phys. Tech.* **76**, 126 (2016).
25. Y. Guo *et al.*, *J. Chem. Phys.* **147**, 104709 (2017).
26. L. Shi *et al.*, *Nanoscale* **10**, 12180 (2018).
27. Q. Zhao *et al.*, *Adv. Funct. Mater.* **28**, 1805304 (2018).
28. V. G. Voevodin *et al.*, *Opt. Mater.* **26**, 495 (2004).
29. D. S. L. Abergel *et al.*, *Appl. Phys. Lett.* **91**, 063125 (2007).
30. M. M. Benameur *et al.*, *Nanotechnol.* **22**, 125706 (2011).
31. S. Yu. Sarkisov *et al.*, *Russ. Phys. J.* **53**, 346 (2010).
32. L. V. Rodríguez-de Marcos *et al.*, *Opt. Mater. Exp.* **6**, 3622 (2016).
33. C. Schinke *et al.*, *AIP Adv.* **5**, 067168 (2015).
34. R. A. Redkin *et al.*, *Russ. Phys. J.* **63**, 1504 (2021).